Hindawi Publishing Corporation
International Journal of Rotating Machinery
Volume 2012, Article ID 823831, 15 pages
doi:10.1155/2012/823831

Research Article

EFD and CFD Design and Analysis of a Propeller in Decelerating Duct

Stefano Gaggero, Cesare M. Rizzo, Giorgio Tani, and Michele Viviani

Department of Electrical, Electronic, Telecommunication Engineering and Naval Architecture (DITEN), University of Genoa, Via Montallegro 1, U16145 Genova, Italy

Correspondence should be addressed to Michele Viviani, viviani@dinav.unige.it

Received 7 September 2012; Accepted 6 November 2012

Academic Editor: Alessandro Corsini

Ducted propellers, in decelerating duct configuration, may represent a possible solution for the designer to reduce cavitation and its side effects, that is, induced pressures and radiated noise; however, their design still presents challenges, due to the complex evaluation of the decelerating duct effects and to the limited amount of available experimental information. In the present paper, a hybrid design approach, adopting a coupled lifting line/panel method solver and a successive refinement with panel solver and optimization techniques, is presented. In order to validate this procedure and provide information about these propulsors, experimental results at towing tank and cavitation tunnel are compared with numerical predictions. Moreover, additional results obtained by means of a commercial RANS solver, not directly adopted in the design loop, are also presented, allowing to stress the relative merits and shortcomings of the different numerical approaches.

1. Introduction

Propeller design requirements are nowadays more and more stringent, demanding not only to provide high efficiency and to avoid cavitation, but including also requirements in terms of low induced vibrations and radiated noise. Ducted propellers may represent a possible solution for this problem; despite the fact that their main applications are devoted to the improvement of efficiency at very high loading conditions (near or at bollard pull), with accelerating ducts, decelerating duct application may result in improved cavitation behavior. Concepts and design methods related to these propulsors are well known since the early 70s [1], and many different works have been presented during years. Notwithstanding the rather long period of application (and study) of these propulsors, their design still presents many challenges, which need to be analyzed, including the evaluation of the complex interaction between duct and propeller, of the duct cavitation behavior, and of its side effects, such as radiated noise and pressure pulses.

These problems are amplified when decelerating, rather than accelerating, duct design is considered; one of the reasons for these difficulties is the higher complexity of the calculation of the duct decelerated flow, which makes the application of conventional lifting line/lifting surface design approaches less practicable or at least not sufficiently accurate. Moreover, a further problem is represented by the lack of experimental data for this type of nozzle configuration with respect to the more conventional (and widely studied) accelerating ones. In order to alleviate the mentioned problems, in the present work, a hybrid design approach is presented. As a first step, the initial estimation of the blade geometry is performed, applying a fully numeric coupled lifting line/panel method solver [2]. Traditional approaches, based on Lerbs approximations [3], are in fact, unable to treat complex geometries, including the effect of the hub and, of course for these kind of propellers, of the duct. A more robust approach is thus required at least for their preliminary design, as well as improved analysis tools, capable to assess the complex viscous interactions that take place on the gap region between the propeller tip and the duct inner surface. This first step geometry is successively refined by means of a panel method coupled

with an optimization algorithm, adopting an approach which already demonstrated successful results in the case of conventional CP propellers [4–6] with multiple design points. In the present case, the use of the panel code in the second design phase (geometry optimization) allows a more accurate evaluation of the cavity extension and of its influence on the propeller performances, thus leading to a better design. The theoretical basis of the design approach is reported in Section 2, while in Section 3 an application to a practical case is presented. Once the final geometry has been obtained, a thorough analysis of the propulsor functioning in correspondence of a wide range of operating conditions, covering design and off-design points (in terms both of load and cavitation indices), is presented. This analysis was carried out applying the same panel method adopted in the design loop and a commercial RANS solver [7] in order to appreciate the capability of the two approaches to correctly capture the ducted propeller performances (mechanical characteristics and cavity inception/extension). If an accurate geometrical description of the duct (within the potential approaches possible only with the employment of the panel method) is fundamental to capture the accelerating/decelerating nature of the nozzles, viscous effects at the duct trailing edge and at the blade tip can have, with respect to the free running propellers case, an even higher influence on the propeller characteristics. The load generated by the duct and the redistribution of load between the blade and the duct itself are, in fact, strongly dependent by the flow regime on the gap region. Sanchez-Caja et al. [8] and Abdel-Maksoud and Heinke [9] successfully predicted the open water characteristics of accelerating ducted propellers with RANS solvers, providing valuable information (beyond the potential codes capabilities) on the features of the flow in the gap region; potential panel methods, in order to simulate these complex phenomena, need the adoption of empirical corrections (like the orifice equation, as in [10]), which may also include the effect of boundary layer on the wake pitch [11] or simplified approaches, like the tip leakage vortex [12]. The accurate description of these phenomena, also through reliable viscous computations, could provide practical ideas for the design process in order to improve the robustness of the approach and the corrections to the potential flow computations. In order to validate the numerical results, an experimental campaign at the towing tank and at the cavitation tunnel was carried out, as presented in Section 4. The comparison of numerical and experimental results in correspondence to the various operating conditions considered allows to stress the merits and the shortcomings of the various approaches, as discussed in Section 5.

2. Theoretical Background

2.1. Coupled Lifting Line/Panel Method Design Approach. In the case of lightly and moderately loaded free running propellers, operating in a nonuniform inflow, the fully numerical design approach is based on the original idea of Coney [2] for the definition, through a minimization problem, of the optimum radial circulation distribution. Traditional lifting-line approaches are, in fact, mainly based on the Betz criteria [3] for the minimum energy loss on the flow downstream of the propeller, and the satisfaction of this condition is realized by an optimum circulation distribution that is generally defined as a sinus series over the blade span. In the fully numerical design approach [2], instead, this continuous radial distribution of vorticity $\Gamma(r)$ along each lifting line that models each of the propeller blades is discretized with a lattice of vortex elements of constant strength. The continuous trailing vortex sheet that represents the blade trailing wake is therefore replaced by a set of M horseshoe vortexes, each of intensity $\Gamma(m)$ and each composed by two helical trailing vortexes, aligned with the hydrodynamic angle of attack and a bound vortex segment, on the propeller lifting line, as in Figure 1.

With this discrete model the influence of the hub can be simply included by means of image vortexes [13], based on the well-known principle that a pair of two-dimensional vortexes of equal and opposite strength, located on the same line, induce no net radial velocity on a circle of radius r_h. The same result approximately holds in the case of three-dimensional helical vortexes, provided that their pitch is sufficiently high. As a consequence, in the case of propellers, the image helical vortexes representing the hub lay on cylinders whose radiuses can be calculated as

$$r_{ih} = \frac{r^2}{r_h}, \tag{1}$$

where r is the radius of each vortex that models the blade, r_{ih} is the radius of its hub images, and r_h is the mean radius of the hub cylinder. This system of discrete vortex segments, bound to the lifting line and trailed in the wake, induces axial and tangential velocity components on each control point of the lifting line, defined as the mean point of each bound vortex segment, where boundary conditions are enforced. These self-induced velocities are computed applying the Biot-Savart law as the contribution, on each control point, of all the horseshoe vortexes modeling each blade:

$$\begin{aligned} u_a(r_i) = u_a(i) &= \sum_{m=1}^{M+M_h} A_{im}\Gamma(m), \\ u_t(r_i) = u_t(i) &= \sum_{m=1}^{M+M_h} T_{im}\Gamma(m), \end{aligned} \tag{2}$$

where A_{im} and T_{im} are, as usual, the axial and tangential velocity influence coefficients of a unit horseshoe vortex placed at the m-radial position on the i-control point (i-radial position) of the lifting line and M and M_h are the total number of horseshoe vortexes representing the blades and their hub images. With this discrete model, the hydrodynamic thrust and torque characteristics of the propeller can be computed by adding the contribution of

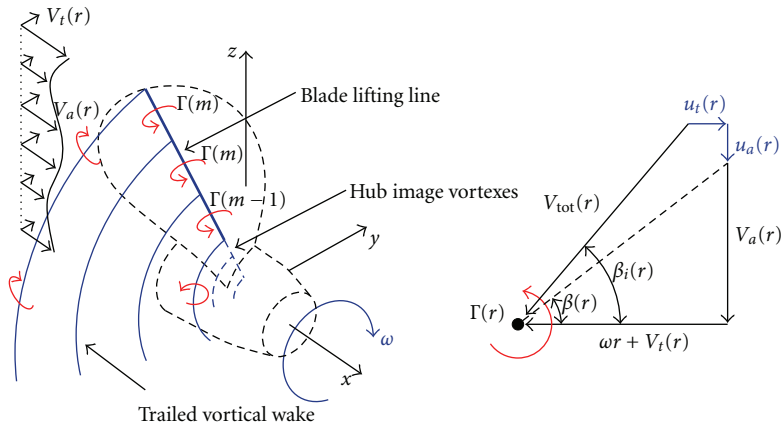

FIGURE 1: Blade equivalent lifting line, reference system, and velocities convention.

each discrete vortex on the line. In fact, under the assumption of pure potential and inviscid flow:

$$T = \rho Z \int_{r_h}^{R} V_{\text{tot}}(r) \cdot \cos\beta_i(r) \cdot \Gamma(r) dr,$$
$$Q = \rho Z \int_{r_h}^{R} V_{\text{tot}}(r) \cdot \sin\beta_i(r) \cdot r \cdot \Gamma(r) dr, \tag{3}$$

where $V_{\text{tot}}(r) \cdot \cos\beta_i(r)$ is simply the total tangential velocity acting at the lifting line (relative inflow $V_t + \omega \cdot r$ plus self-induced tangential velocity u_t), $V_{\text{tot}}(r) \cdot \sin\beta_i(r)$ is the axial velocity (inflow V_a plus self-induced axial velocity u_a), and β_i is the hydrodynamic pitch angle. In discrete form (3) leads to

$$T = \rho Z \sum_{m=1}^{M} [V_t(m) + u_t(m) + \omega \cdot r] \cdot \Delta r \cdot \Gamma(m),$$
$$Q = \rho Z \sum_{m=1}^{M} [V_a(m) + u_a(m)] \cdot r(m) \cdot \Delta r \cdot \Gamma(m). \tag{4}$$

A variational approach [2] provides a general procedure to identify the set of discrete circulation values $\Gamma(m)$ (i.e., the radial circulation distribution for each propeller blade described as the superposition of the strength of its M horseshoe vortexes) such that the propeller torque (as computed in (4)) is minimized, keeping contemporarily to a constant value (within a certain tolerance) the required propeller thrust T_R, which is a constrain of the problem. Introducing the additional unknown represented by the Lagrange multiplier λ, the problem can be solved in terms of an auxiliary function $H = Q - \lambda \cdot (T - T_R)$, requiring that its partial derivatives are zeros:

$$\frac{\partial H}{\partial \Gamma(m)} = 0, \quad \text{for} \quad m = 1 \cdots M,$$
$$\frac{\partial H}{\partial \lambda} = 0. \tag{5}$$

Carrying out the partial derivatives, (5) leads to a nonlinear system of equations for the vortex strengths and for the Lagrange multiplier, because self-induced velocities depend, in turn, on the unknown vortexes strengths themselves. The iterative solution of the nonlinear system is obtained by the linearization proposed by Coney [2] in order to achieve the optimal circulation distribution that minimizes torque with the prescribed thrust.

This formulation can be further improved to design moderately loaded propellers and to include viscous effects. The initial horseshoe vortexes that represent the wake, frozen during the solution of (5), can be aligned with the velocities induced by the actual distribution of circulation and the solution iterated until convergence of the wake shape (or of the induced velocities themselves).

A viscous thrust reduction, as a force acting on the direction parallel to the total velocity and thus as a function of the self-induced velocities themselves, can be furthermore added to the auxiliary function H, and a further iterative procedure, each time the chord distribution of the propeller has been determined, can be set. In total, for the design of a single propeller, the devised procedure works with

(i) an inner iterative approach for the determination of the optimal circulation distribution by the solution of the linearized version of (5),

(ii) a second-level iterative approach to include the viscous drag on the optimal circulation distribution, by adding viscous contribution to the auxiliary function H,

(iii) a third-level iterative approach to include the wake alignment and the moderately loaded case.

This design procedure outlined for free running propellers can be easily extended to treat the case of ducted propellers. As for the hub, the influence of the nozzle on the performances of the propeller can be included in the numerical lifting line model simply adding an appropriate set of image vortexes in place of the duct itself, in order to include its "wall" effect and the resulting loading of the blade tip region. With a formulation equivalent to that of (1), it is possible to define the radial location of the duct image

vortexes, replacing the hub cylinder mean radius r_h with the duct cylinder mean radius r_d.

The presence of the duct, however, influences the propeller performances not only in terms of additional load at the tip. The shape of the nozzle (for accelerating or decelerating configurations) induces very different inflow distributions on the propeller plane, which cannot be taken into account by means of the simple addition of the image vortexes that model the "wall" condition. The main responsibles of the modified inflow at the propeller plane are, in fact, the effective shape and the thickness of the nozzle that are neglected by the vortical approach. Moreover the nozzle contributes to the total propulsive thrust, and, therefore, the design of a ducted propeller has to include this additional term. To overcome the limitation of the original approach based only on a distribution of vortexes, an iterative methodology has been devised, in order to couple the numerical lifting line design approach (for the determination of the optimal circulation distribution and of the resulting propeller geometry) with a panel method, suited for a more accurate computation of the inflow velocity distribution on the propeller plane and for the evaluation of the duct thrust force. The coupling strategy between the two codes is schematically presented in Figure 2. With respect to the procedure outlined in the case of free running propellers, the coupling with the panel method modifies the inner and the outer iterative loops. The interaction between the propeller lifting line and the duct is, in fact, achieved through induced velocities. Every time a new circulation distribution has to be computed, the panel method provides the input inflow velocity distribution V_a and V_t necessary in (4) and the definition of the hydrodynamic pitch angle β_i needed for the determination of the trailing vortexes shape on the propeller wake. The duct (without the propeller), operating on the mean inflow generated by the set of lifting line vortexes computed at the previous design iteration, is solved by the panel method, and the mean axial and tangential velocities induced on the propeller plane are used as the input inflow for the next design step. Furthermore, once a propeller geometry has been defined, not only the frictional forces are computed and the propeller thrust is updated but also the duct thrust/resistance is calculated (by the panel method applied to the entire propeller/duct problem) and the required propeller thrust is adjusted in order to achieve the total (propeller plus duct) propulsive thrust.

After the blade circulation and hydrodynamic pitch distribution have been defined, the design procedure proceeds to determine the blade geometry in terms of chord length, thickness, pitch, and camber distributions which ensure the requested sectional lift coefficient satisfying, at the same time, cavitation and strength constraints. For the calculation of blade stresses the method proposed by Connolly [14] has been preferred, while cavitation issues are solved in accordance with the approach developed by Grossi [15], in turn based upon an earlier work by Castagneto and Maioli [16] where minimum pressure coefficients on a given blade section with standard NACA shapes are semiempirically derived. A more detailed description of the design procedure may be found in Gaggero et al. [17, 18].

2.2. Design by Optimization. The design of ducted propellers via lifting line approaches remains, however, problematic. Despite the lifting surface corrections that can be adopted for the definition of the blade geometry (through the empirical corrections proposed by VanOossanen [19] or by a dedicated lifting surface code), the influence of the blade and of the duct thickness, the nonlinearities linked with the cavitation, and the effects of the flow in the gap between the blade tip and the inner duct surface strongly affect the optimal propeller geometry. An alternative and successful way to improve the propeller performances is represented by optimization [4–6]. The design of the ducted propeller can be improved, in fact, adopting an optimization strategy, namely, testing thousands of different geometries, automatically generated by a parametric definition of the main geometrical characteristics of the propeller (eventually also of the duct), and selecting only those able to improve the performances of the initial configuration (e.g., in terms of efficiency and cavity extension) together with the satisfaction of defined design constraints (thrust identity, first of all).

Panel methods, with their extremely high computational efficiency (at a sufficient level of accuracy with respect to RANS solvers), are the natural choice for the analysis of thousands of geometries: with respect to lifting line/lifting surface models, panel methods allow to directly compute the influence of the hub and, especially, of the duct, both in terms of the additional load on the blade tip region and in terms of the velocity disturbance on the whole propeller, avoiding the simplified representation of the duct only by vortex rings and sources. Also cavitation (at least sheet cavitation both on the back and on the face blade sides) can be directly taken into account, by means of a better computation of the pressure distribution instead than by semiempirically derived minimum pressure coefficients on standard blade sections.

For the improvement of the ducted propeller performances a panel method developed at the University of Genoa [20, 21] and specifically customized for the solution of cavitating ducted propellers with the inclusion of the tip gap flow corrections [10] has been adopted. Potential solvers are based on the solution of the Laplace equation for the perturbation potential ϕ [22], which is the counterpart of the continuity equation if the hypotheses of irrotationality, incompressibility, and absence of viscosity are assumed for the flow:

$$\nabla^2 \phi = 0. \tag{6}$$

Green's second identity allows to solve the three-dimensional problem of (6) as a simpler integral problem involving only the surfaces that bound the computational domain. The solution is found as the intensity of a series of mathematical singularities (sources and dipoles) whose superposition models the inviscid, cavitating flow on and around the propeller. Boundary conditions (dynamic and kinematic both on the wetted and the cavitating surfaces, Kutta condition at the trailing edge, and cavity bubble closure at bubble trailing edge) close the solution of the linearized system of equations obtained from the discretization of the differential problem represented by (6) on a set of

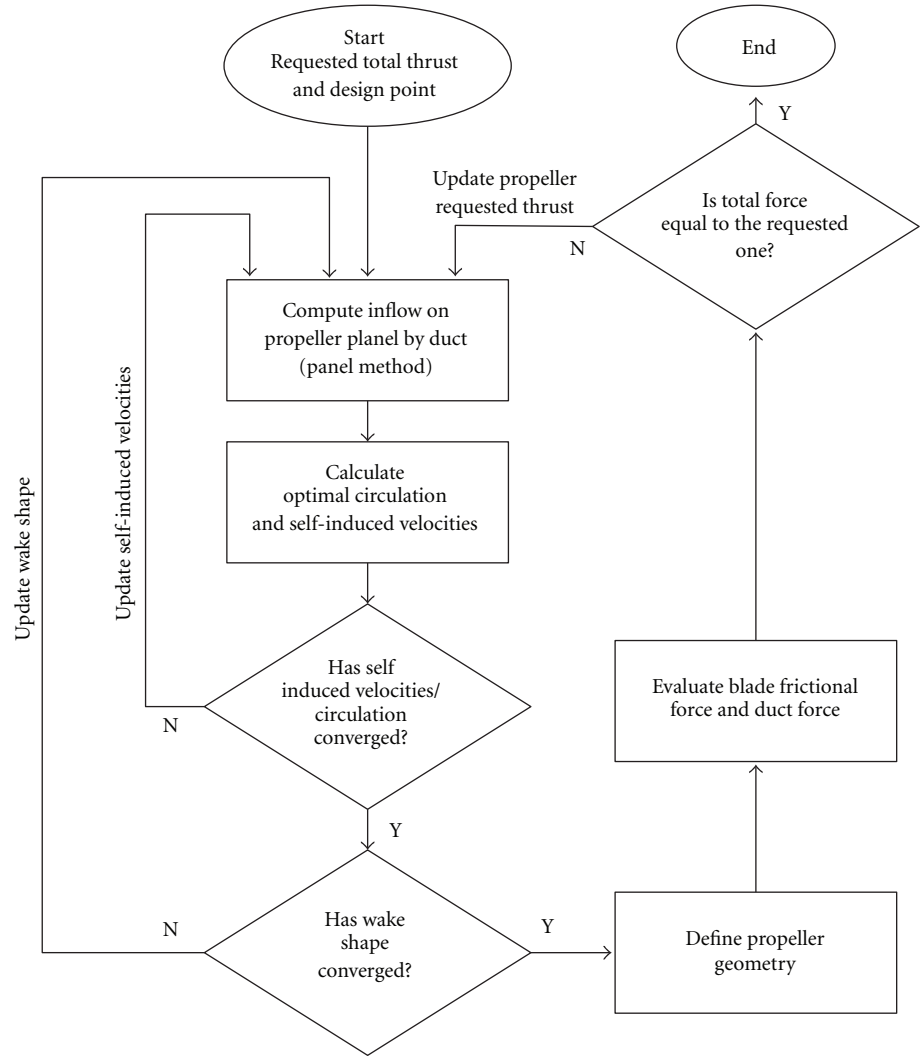

Figure 2: Flow chart for the coupled lifting line/panel method design approach.

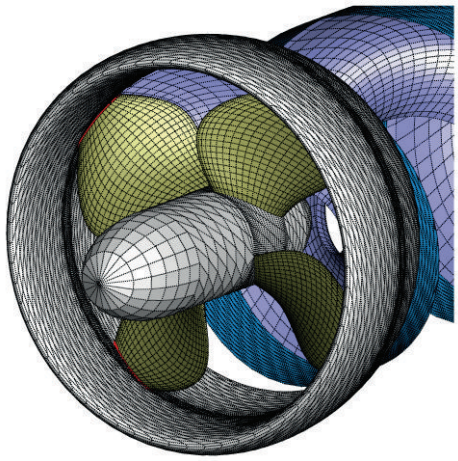

Figure 3: Panel representation of the ducted propeller. Tip gap region in red.

hyperboloidal panels representing the boundary surfaces (Figure 3) of the hub, the blade, the duct, and the relative trailing wakes. An inner iterative scheme solves the nonlinearities connected with the Kutta boundary condition while an outer cycle solves the nonlinearities due to the unknown cavity bubble extension. As usual forces are computed by integration of the pressure field, evaluated by the Bernoulli theorem, over the propeller surfaces, while the effect of viscosity is taken into account with a standard frictional line correction. With respect to the free running propeller case, the solution of the potential problem, when a ducted propeller is addressed, requires a special treatment of the flow on the gap region that could strongly influence the propeller tip loading and the distribution of load between the propeller and the duct itself. In present case a gap model with transpiration velocity (similar to that proposed by Hughes [10]) and the orifice equation are adopted. At first an additional strip of panels along the blade tip is introduced to close the gap between the propeller and the duct. Moreover, a wake strip of panels is added, for which

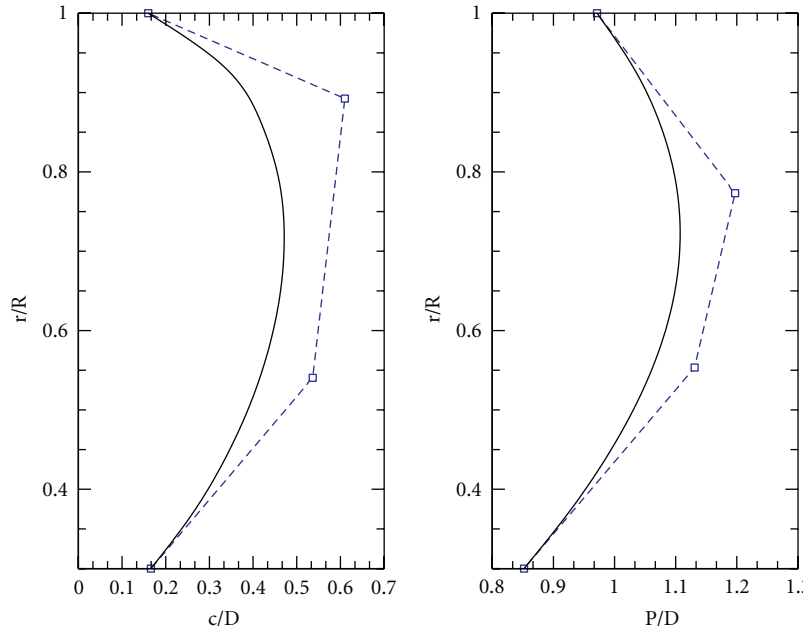

Figure 4: B-Spline representation of radial distributions of chord and pitch.

Figure 5: Polyhedral mesh arrangements for the ducted propeller—open water computations.

the dipole strength is determined again from the Kutta condition. The existence of a transpiration velocity through the gap is obtained with a modification of the kinematic boundary conditions ($\partial\phi/\partial n = -V_\infty \cdot n$ for fully wetted panels) applied to the panels on the gap strip:

$$\frac{\partial\phi}{\partial n} = -V_\infty \cdot n + |V_\infty| \cdot C_Q\sqrt{\Delta C_P} \cdot n \cdot n_c, \qquad (7)$$

where n_c is the unit normal vector to the mean camber line at the gap strip on the same chordwise position of the panel, n is the unit normal of each panel on the gap strip, V_∞ is the total, local velocity vector, C_Q is an empirical discharge coefficient (set equal to 0.85) to take into account the losses on the gap region, and ΔC_P is the unknown pressure difference between the face and back side of the gap region. A further iterative scheme is, thus, required to force the boundary condition of (7) on the gap panels: as a first step, the problem is solved as if the gap was completely closed ($C_Q = 0$), and the initial pressure difference is computed; in following steps, (7) is updated with the current value of pressure difference, and the potential problem is solved again until a certain convergence of the gap flow characteristics is achieved.

For the application of the panel method (mainly an analysis, not a direct design code) into a design procedure through optimization, a robust parametric representation of the propeller geometry [4–6, 20, 21] is needed. The classical design table is, inherently, a parametric description of the geometry itself. All the main dimensions that define propeller geometry, like pitch, camber, and chord distribution along the radius, represent main parameters that can easily be fitted with B-Spline parametric curves, whose control points turn into the free variables of the optimization procedure, as in Figure 4. As regards the profile shape, instead of adopting standard NACA or Eppler types, with the same parametric approach it is possible to describe with only few control points thickness and camber distribution along the chord for a certain number of radial sections (or, more consistently, to adopt a B-Surface representation of the mean nondimensional propeller surface) and include also profiles in the optimization routine.

The adopted optimization algorithm is of genetic type: from an initial population (whose each member is randomly created from the original geometry, altering the parameter values within prescribed ranges), successive generations are created via crossover and mutation. The members of the new generations arise from the best members of the previous one that satisfy all the imposed constraints (e.g., thrust identity)

and grant better values for the objectives. To improve the convergence of the algorithm and speed up the entire procedure, a certain tolerance (within few percent points) has been allowed for the constraints, letting the inclusion of some more different geometries in the optimization loop. In particular, in the specific case presented in Section 3, thrust coefficient variations of ±2% have been accepted. Each member of the initial population is analyzed via the potential code. Results, in terms of thrust, torque, efficiency, and cavity area, are collected together with the values of the parameters that describe that given geometry. The optimization algorithm, through these data, identifies the "direction" to be followed in order to satisfy the constraints and improve the objectives until convergence is achieved (or Pareto convergence in the case that more than one objective are addressed).

2.3. Analysis Tools. Panel methods can accurately take into account the thickness effect, the nonlinearities due to cavitation, and, even if in an approximate way, the interaction between the propeller and the nozzle, in terms both of increase of loading at the tip and inflow velocity distribution. For these reasons the optimization has been carried out performing all the calculations with a panel method customized for the solution of the ducted propeller problem. On the other hand the accuracy and the efficiency of RANS solvers has increased significantly in the last years (see, e.g., [17, 18] and, for the ducted propellers, [8, 9]), making RANS solutions, in many engineering cases, a reliable alternative to the experimental measurements and an excellent tool to understand and visualize, for instance, the complex flow phenomena on the gap region. In addition to the panel method, hence, also a commercial finite volume RANS solver, namely, StarCCM+ [7] has been adopted to evaluate the performances and the characterizing flow features (tip vortexes and cavitation) of ducted propellers and, thereby, to have a further set of results to be compared with the experimental measures. For the noncavitating computations, as usual continuity and momentum equations for an incompressible fluid are expressed as

$$\begin{aligned} \nabla \cdot V &= 0, \\ \rho \dot{V} &= -\nabla p + \mu \nabla^2 V + \nabla \cdot T_{\mathrm{Re}} + S_M \end{aligned} \tag{8}$$

in which V is the averaged velocity vector, p is the averaged pressure field, μ is the dynamic viscosity, S_M is the momentum sources vector, and T_{Re} is the tensor of Reynolds stresses, computed in agreement with the two-layer realizable k-ε turbulence model. In the case of cavitating flow an additional transport equation for the fraction α of liquid is needed: continuity and momentum equations are solved for a mixed fluid whose proprieties are a weighted mean between the fraction α of liquid and the fraction $1 - \alpha$ of vapor. In turn also continuity equation is modified, in order to take into account the effect of cavitation through a source term, modeled by the Sauer and Schnerr [23] approach.

The numerical solutions have been computed on appropriate meshes (e.g., Figures 3 and 5), whose reliability has been verified similarly to Bertetta et al. [4–6].

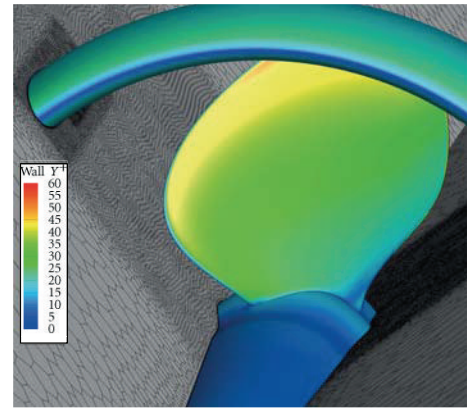

Figure 6: Wall Y^+ on propeller and duct—open water computations at the design condition.

As it is well known, the quality of the mesh is a decisive factor for the overall reliability of the computed solution. From this point of view, automatic unstructured meshes, as those adopted in the present case, may pose some additional issues with respect to the more user adjustable structured ones. To limit the numerical errors and to grant smooth variations of the geometrical characteristics of the cells, where local refinements (adopted to increase the accuracy where the most peculiar phenomena of these kind of propellers are expected) have been adopted, special attention has been dedicated to define the appropriate growing factors that drive the transition of the cells dimensions and of the prism layers arrangement. For instance, depending on whether the computation is for the open water or for the cavitating condition, different modellings of the prism layer have been adopted, in the light of the local Reynolds number (i.e., turbulent layer thickness) of the model propeller tested (diameter of 230 mm) at the cavitation tunnel and of an estimated (panel method) sheet cavity thickness. The main parameters for both the computations are summarized in Table 1. The adopted mesh, as usual, is a compromise between accuracy and available computational time. In any case all the parameters that define the quality of the mesh fall within the thresholds (e.g., volume change greater than $1 \cdot 10^{-5}$ and maximum skewness angle lower than 85°) suggested for reliable solutions on unstructured polyhedral meshes [7]. The dimensionless wall distance, as also presented in Figure 6 for the noncavitating propeller at the design point, is overall adequate for the application of the selected two-layer realizable k-ε turbulence model.

Moving reference frames (for RANS computations) and key blade approaches (in the framework of the potential approach, as in Hsin [24]) have been finally adopted to exploit the axial symmetry of the problem and reduce the computational domain.

3. Design Activity

The coupled lifting line/panel method design methodology and the design via optimization outlined in the previous

Table 1: Main discretization parameters.

	Open water	Cavitating flow
Panel method		
Number of panels	About 3200	About 3200
Time step(s)	Steady computation	Steady computation
RANS		
Number of cells	About 2.7 millions	About 3.3 millions
Number of prism layers	5	10
Prism layer thickness (mm)	0.8	1.5
Y^+ (average on blade)	Abt. 35	Abt. 35
Y^+ (average on duct)	Abt. 25	Abt. 25
Y^+ (max at blade trailing edge)	73	95
Y^+ (max at duct trailing edge)	47	59
Max. skewness angle	Abt. 73	Abt. 83
Min. volume change	$4 \cdot 10^{-4}$	$3.6 \cdot 10^{-4}$
Time step(s)	Steady computations	$5 \cdot 10^{-5}$

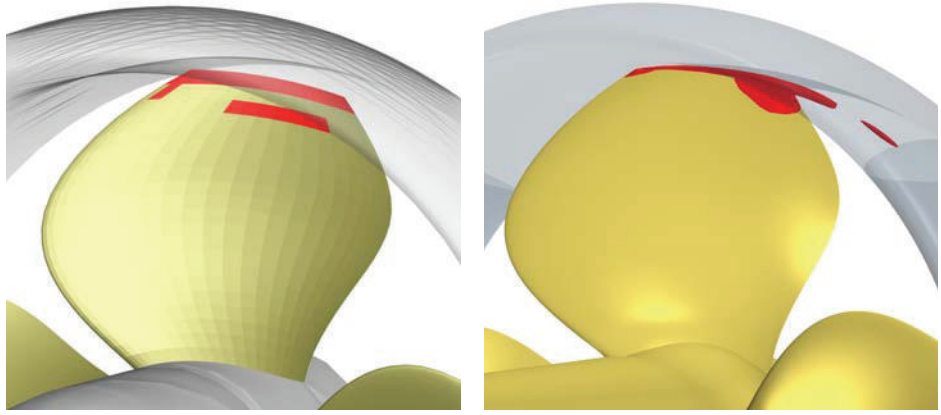

(a) (b)

Figure 7: Predicted cavity extension for the preliminary propeller geometry at the design advance coefficient. (a) Panel method computations at 90% of the design cavitation index. (b) RANS computations at the design cavitation index.

sections have been employed for the definition of an optimal four-blade decelerating ducted propeller operating in moderately loaded conditions. The duct is shaped as an NACA profile, and its geometry, given for the preliminary design through the lifting line/panel method procedure, has been maintained unaltered also for the optimization. The complete details of nozzle geometry may not be provided for industrial reasons. A prescribed total (propeller plus duct) thrust coefficient, to be satisfied at an advance coefficient close to 1 and at a cavitation index (based on the number of revolutions) of about 1.5, has been assumed for the design of the propeller.

The resulting preliminary geometry (having a pitch over diameter ratio at 0.7 radial section of about 1.33) from the coupled lifting line/panel method design procedure is presented in Figure 7, in which both the panel method and the RANS results in terms of predicted cavity extension are shown. The agreement between the numerical results from both the approaches is satisfactory, showing similar cavitation extents. In terms of predicted thrust, the effectiveness of the design is confirmed by the numerical computations. The value predicted by the RANS is very close (about 2% lower) to the required total thrust assumed for the design; this discrepancy was deemed acceptable. The numerical predictions of the thrust and of the torque obtained with the panel method for the same preliminary geometry show, instead, some differences with respect to the RANS computations: panel method results tend to be a bit more overpredicted, with respect to the required total thrust and, as a consequence, with respect to the RANS calculations. For the optimization it has been assumed that these differences, ascribed to the numerical approach, remain the same also for the newly designed propellers, and the numerical predictions by the panel method obtained for

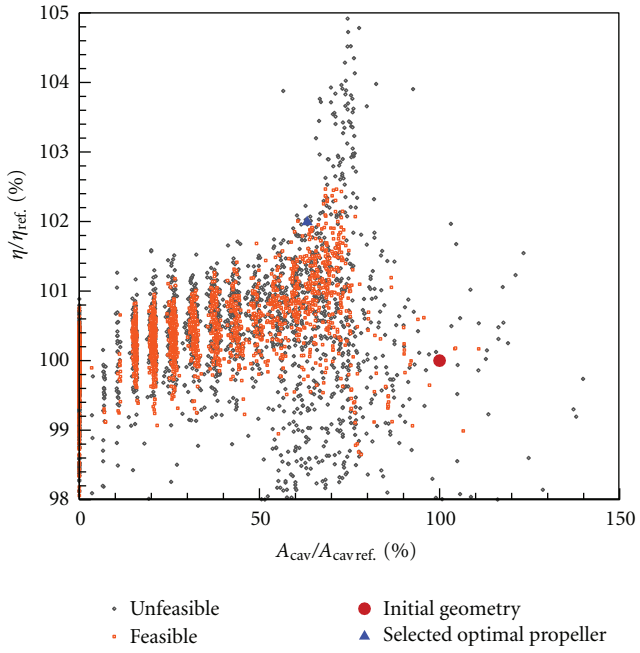

Figure 8: Pareto designs with preliminary (red) and final (blue) propellers numerical performances.

the preliminary propeller designed with the coupled lifting line approach have been taken as the reference point of the optimization procedure.

Starting from this preliminary geometry, the optimization of the propeller has been carried out in order to obtain a new geometry able to maximize efficiency and to reduce back cavitation at the design cavitation index with the same numerical delivered thrust (within a range of ±2% to speed up the convergence) computed for the preliminary design.

Also in terms of cavity extension, some limitations of the panel approach can be highlighted. Previous experiences at the cavitation tunnel with similar decelerating ducted propellers (and also the viscous computations on the preliminary geometry as presented in Figure 7) showed that tip leakage vortex, whose prediction is, of course, beyond the capabilities of the cavitating panel method, is one of the dominating cavitating phenomena. If for the RANS the prediction of cavitating vortexes can be considered reliable, for the panel method it is clear that only an artificial sheet cavity bubble is computed on the outermost strip of panels at tip. This sheet cavitation, that has been numerically evidenced at the blade tip could be, however, correlated (this assumption will be partially confirmed by the experimental campaign) with the occurrence of the tip cavitating vortex, and its extension (to be, as a consequence, minimized) could be considered a measure of the risk (or strength) of this kind of cavitation. The risk of midchord bubbles at tip is, moreover, evidenced by both methods: the RANS vapor isosurface (fraction of vapor equal to 0.5) covers the blade at its trailing edge just below the tip while; by the panel method, again a sheet cavity bubble is predicted at midchord near the same position. In order to numerically amplify the sheet cavity bubble at the blade tip, include a certain margin for the occurrence of bubble cavitation and let the optimization work at a more convenient point (for which the cavity extension is not constrained by the dimension of the few panels at the blade leading edge); the design of the new propeller via optimization has been carried out at a slightly lower cavitation index with respect to the design point (90%), as mentioned also in Figure 7.

The optimization activity for the design of the new propeller has been carried out investigating only global parameters, that is, maintaining the profile shape adopted for preliminary design. In particular chord, maximum camber and pitch distributions along the radius have been considered in the optimization, taking control points of the related curves as free variables. Maximum thickness has been constrained to the chord distribution in order to achieve the same blade strength of the initial propeller.

About 20 thousands different geometries have been generated and analyzed by the panel method; results of the optimization are reported in the Pareto diagram of Figure 8. Feasible geometries are those that satisfy all the prescribed constraints (thrust identity for instance) while unfeasible points represent the performances, in terms of efficiency and cavity extension, of the geometries that do not satisfy the constraints.

One of the most powerful aspects of the optimization is the availability, at the end of the design process, of an entire set of geometries, all satisfying the design criteria (within the limits of the adopted flow solvers) with different compromises regarding the design objectives. Among the Pareto frontiers, thereby, it is possible to select a new geometry, as a balance between increase of efficiency and reduction of cavity extension also in the light of the designer experience. The new optimal geometry (having a pitch over diameter ratio at 0.7 radial section of about 1.32), as highlighted in Figure 8, grants a numerical reduction of the cavity extension of about 40% and an increase in efficiency slightly greater than 2% at the same working point of the preliminary geometry, and, as expected, the total thrust computed by the panel method is within the prescribed numerical tolerance of ±2%. Also for the optimal geometry a more accurate RANS computation has been carried out, whose results, in terms of predicted cavity extension, are reported in Figure 9. As wished, RANS results confirm the effectiveness of the optimization approach: the total propeller thrust of the optimized propeller is, as well as the total thrust of the preliminary design, 2% lower than the requested design thrust, with an efficiency 1.8% greater than that computed by the RANS in the case of the preliminary design. The predicted RANS cavity extension is itself in agreement with the panel method analysis (with the limits already underlined by the analysis of the cavity prediction of the preliminary design), and, at least qualitatively, it is possible to evidence a nonnegligible reduction with respect to the same kind of numerical analysis presented in Figure 7 for the preliminary geometry.

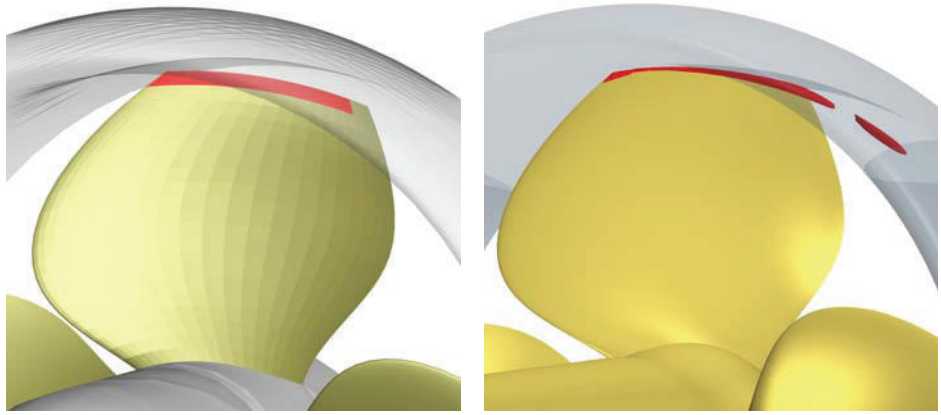

(a) (b)

Figure 9: Predicted cavity extension for the optimized propeller geometry at the design advance coefficient. (a) Panel method computations at 90% of the design cavitation index. (b) RANS computations at the design cavitation index.

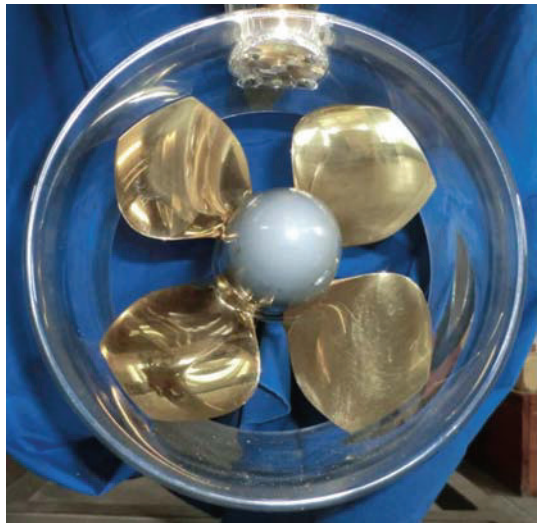

Figure 10: Ducted propeller model.

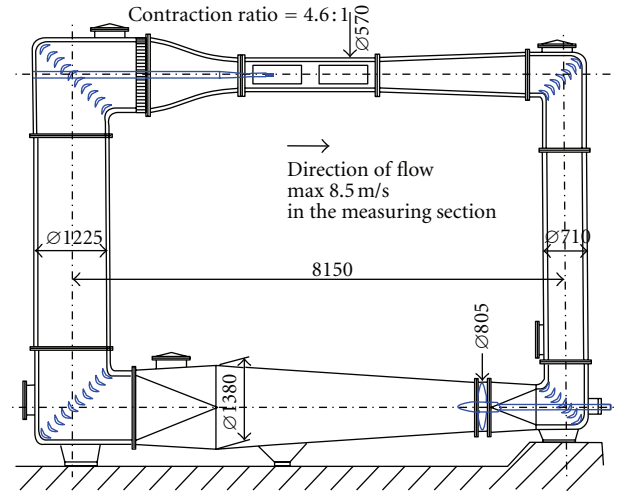

Figure 11: University of Genoa Cavitation Tunnel.

4. Experimental Campaign

Once the final geometry has been chosen, a series of model tests (open water tests and cavitation tunnel tests) has been performed in order to validate the numerical results. The model used throughout the tests (having a diameter of 230 mm) is reported in Figure 10.

In particular, open water tests have been carried out at SVA towing tank, using a Kempf & Remmers propeller dynamometer H39 and a R35X balance for the measurement of duct thrust. A constant propeller rate of revolution (15 Hz) was adopted during tests.

Cavitation tunnel tests have been carried out, instead, at the University of Genoa cavitation tunnel. The facility, represented in Figure 11, is again a Kempf & Remmers closed water circuit tunnel with a squared testing section of 0.57 m $\times$ 0.57 m, having a total length of 2 m, in which conventional propeller cavitating behaviour [25] and SPP propellers characteristics [26] are usually tested.

The nozzle contraction ratio is 4.6 : 1, and the maximum flow speed in the testing section is 8.5 m/s. Vertical distance between horizontal ducts is 4.54 m, while horizontal distance between vertical ducts is 8.15 m. Flow speed in the testing section is measured by means of a differential venturimeter with two pressure plugs immediately upstream and downstream of the converging part. A depressurization system allows obtaining an atmospheric pressure in the circuit near to vacuum, in order to simulate the correct cavitation index for propellers and profiles. The tunnel is equipped with a Kempf & Remmers H39 dynamometer, which measures the propeller thrust, the torque, and the rate of revolution.

Figure 12: Measurement setup at cavitation tunnel.

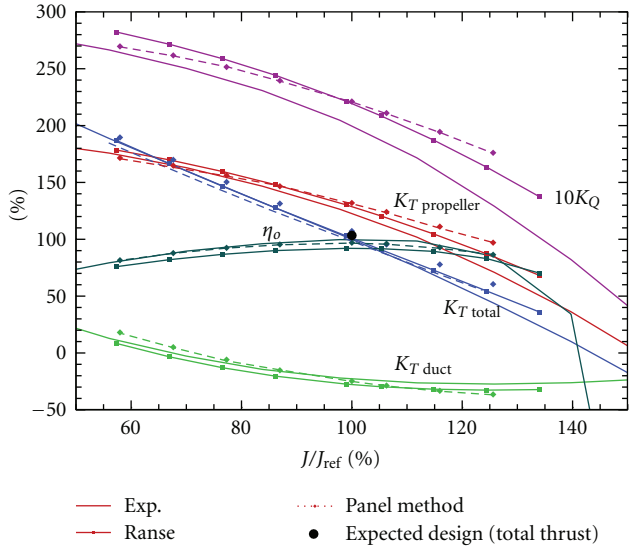

Figure 13: Non-dimensional open water propeller characteristics.

As usual, a mobile stroboscopic system allows to visualize cavitation phenomena on the propeller blades. Moreover, cavitation phenomena visualization in the testing section is also made with two Allied Vision Tech Marlin F145B2 Firewire Cameras, with a resolution of 1392 × 1040 pixels and a frame rate up to 10 fps. As regards the duct forces, an in-house developed measuring device has been adopted. In particular, a cavitation tunnel window was modified to hold an aluminium alloy plate coupled by welding to an aluminium alloy hollow bar [27]. Force measurement is performed by means of strain gauges directly applied on the hollow bar. This instrumentation was successfully tested against towing tank results, as reported in Bertetta et al. [4–6], where further details about its development and calibration may be also found.

In order to avoid vortex shedding from the hollow bar in the tunnel flow, which can affect bar integrity and decrease dramatically its fatigue life, a screening foil was adopted. The foil shape was selected in order to postpone cavitation, thus limiting, as far as possible, the additional noise due to the presence of the measuring device. In Figure 12 the final measurement setup at cavitation tunnel is shown.

All tests were carried out without axis longitudinal inclination and in an uniform wake, consistently with the design assumptions previously described. A constant propeller rate of revolution (25 Hz) was adopted.

5. Comparison of Numerical and Experimental Results

5.1. Open Water. Model scale open water computations, compared with measures carried out at SVA towing tank, are shown in Figure 13. Results are reported in nondimensional form, with the normalization carried out with respect to the towing tank values at the design point.

Measures substantially confirm the design procedure. The optimized propeller, at the design point, has a slightly lower (about 3%) thrust with respect to that required during the design. The RANS computations, which were assumed as a validation of the preliminary and the optimized designs (predicting values of total thrust 2% lower than that assumed for the design, as in the previous section), are very close to the experimental point, with a discrepancy (overestimation) in terms of the total thrust less than 1%.

Since calculations have been carried out in correspondence to a rather large range of advance coefficient values, not limiting to the design point, it is worth discussing them, examining in particular the existing discrepancies.

Considering thrust coefficients, RANS computations can be considered, also in off-design, sufficiently reliable. Particularly at lower values of advance the agreement between the measured and the computed total (propeller plus nozzle) thrust is good, even if it has to be remarked that the propeller thrust is slightly overestimated while the nozzle one is slightly underpredicted, with their sum very close to the experiments as a counterbalance of two diverging errors. Only for higher values of advance, thrust predictions are significantly different from the measures, confirming the very complex nature of flow inside highly loaded decelerating nozzles. This difference may be mainly due to a progressively increasing error in the prediction of the propeller thrust alone, probably due to a noncompletely satisfactory modelling of the mutual interaction between duct and propeller. Discrepancies in torque prediction (and, in turn, in efficiency) are, instead, more evident. At the design point the numerical overestimation is about 10%, but the torque curve is almost constantly vertically shifted with respect to the experimental measures. Unfortunately, panel method predictions amplify the discrepancies already highlighted for the RANS. Even if at lower advance coefficients total thrust values (as a counterbalance of propeller and nozzle thrust predictions) are deemed acceptable, with a 7% difference at the design point; at higher advances the differences with the measures increase, confirming the limitations of the adopted panel method when applied to solve the complex flow phenomena that occur, for instance, on the gap region. Discrepancy in the torque coefficient is comparable to those

obtained with RANS at design point, with differences in off-design conditions which are in line with thrust coefficient behaviour.

As already mentioned, the discrepancies between numerical results and measurements may be due to the noncorrect capturing of the flow in the decelerating duct. Previous calculations with RANS and panel method on a propeller with accelerating duct, in fact, provided lower discrepancies (similar to those found in [9, 11]) in correspondence to the functioning points at lower values of advance coefficient, where an accelerating effect exists, while higher discrepancies were found when duct functioning is reversed, that is, when a decelerating effect is present. Unfortunately, decelerating duct configurations are scarcely considered in literature, especially for what regards numerical calculations, limiting the possibility of comparisons.

Notwithstanding this problem, the quality of present results, despite presenting considerable discrepancies especially in terms of torque coefficient, is deemed acceptable in the context of the proposed design procedure, since it showed to be able to rank different propellers. In particular, three different geometries with same decelerating duct were numerically and experimentally tested in a parallel activity. The relative trends, in terms of efficiency, were correctly captured by both panel and RANS methods, which succeeded in ranking correctly the three different propellers, with panel methods slightly amplifying the differences found with experiments and RANS slightly smoothing them. Complete results may not be included for industrial reasons. Currently, in the context of the propeller design activity, the presented calculations parameters were therefore considered a correct compromise between calculations accuracy and required computational time.

In order to have a better insight into the problem, a first analysis with RANS has been carried out considering the possible influence of turbulence models. In particular, k-ω and RST turbulence closure equations were adopted, keeping constant mesh parameters. The results did not present significant modifications and are therefore omitted. Possible further analyses, which will be carried out in future activities, will consider the influence of the adoption of more refined meshes and of structured grids, with the aim of better capturing flow features in the small gap region.

Regarding panel method, a possible future improvement can be represented by the introduction of a better trailing wake model, as proposed by Baltazar et al. [11].

5.2. Cavitating Conditions. The cavity extension observed at the cavitation tunnel of the University of Genoa has been compared with the numerical computations carried out with the panel method and the RANS solver. Four different functioning points, in addition to the design one, have been considered. Two of the four points have the same design thrust coefficient and different cavitation indexes while the other two have the same cavitation index but increased and decreased value of the thrust coefficient. All the comparison have been carried out at the same (experimental and numerical) thrust coefficient in order to minimize the discrepancies between measures and numerical computations highlighted for the open water case. As a first step, cavitation extension at design point is considered. Results are shown in Figure 14: cavitating tip leakage vortex is the only noticeable phenomenon, which extends on the duct.

A satisfactory agreement is found between the experimentally observed phenomena and the RANS numerical calculation, which show that the propeller is cavitation-free, except for the tip leakage vortex, whose existence is captured. Moreover, numerical tip vortex shows also a pitch very similar to the observed one, which is considerably lower than it would be expected in case of a conventional propeller. This feature is probably due to the local effect of the duct wake and of the flow in the gap region. Nevertheless, the numerically predicted extension of the cavity area appears larger than the experimental one, which develops only from about midchord. It is important to underline that the vortex appeared considerably unstable during the experiments, with a variable extension (the photograph presented may be considered as a mean value). This instability, which is strongly influenced by local characteristics of the propeller (including tip geometry and tip gap), was particularly evident in correspondence to the design point, while it decreased at lower and higher loadings of the propeller. Panel method results are also satisfactory, showing no cavitation on propeller blade apart from a very limited number of panels at the tip, which may be considered as an indication of the existence of the tip leakage vortex, which may not be captured by the method by its nature. As a whole, therefore, the results confirm the reliability of the adopted design procedure, which allowed to obtain an almost completely cavitation-free propeller, apart from the tip leakage vortex. It has to be noted however that, as well known, the cavitating tip vortex may be problematic, especially if the aim of the designer is the reduction of noise level. Future analyses will be carried out in order to compare the peculiar tip leakage vortex effect with typical conventional propeller noise levels and to analyze factors (propeller geometry at tip, propeller/duct clearance, effective flow) linked to the generation and behavior of this phenomenon. Off-design comparisons are shown in Figures 15 and 16, obtained from varying the cavitation number at the same design thrust coefficient, and in Figures 17 and 18, obtained from different loadings at the same design cavitation number.

Again, having in mind the intrinsic limitations of the numerical approaches, a satisfactory agreement with experiments can be evidenced. In particular, panel method allows to rank, by means of the number of cavitating panels at the tip, the strength of the tip leakage vortex. A very good correlation exists, in fact, between the evaluated cavitation extension and the dimension of the tip leakage vortex; the unique functioning condition in which no cavitating panel is present is the one with lower loading, where the tip leakage vortex is effectively very weak. This consideration allows to state that panel method, at least to some extent, may be adopted, beyond its usual application, also as a tool to reduce (coupled with optimization techniques) the tip leakage vortex. However, this consideration has to be further investigated, since it is likely that, once differences

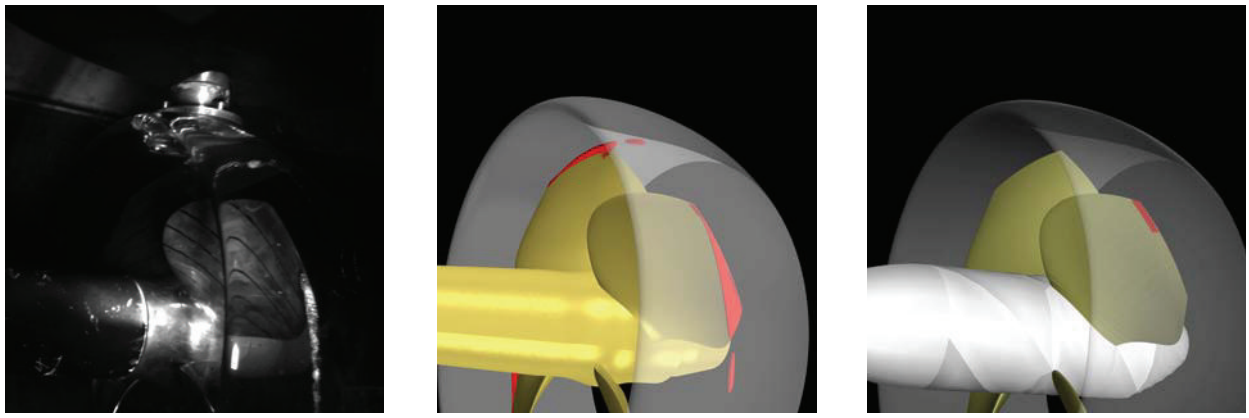

Figure 14: Observed and predicted (RANS and panel method) cavity extension at the design point.

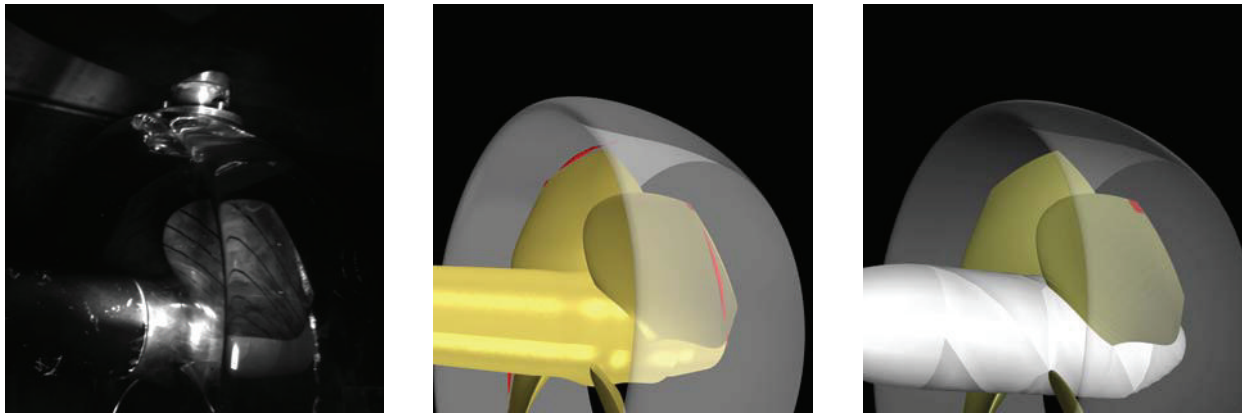

Figure 15: Observed and predicted (RANS and panel method) cavity extension. Design thrust coefficient at 135% of design cavitation index.

at tip reduce to small details, panel methods would fail in rank different solutions. Calculations with RANS, which show again a very good general agreement with experimental observations, might be a more reliable alternative if interest is posed on the tip leakage vortex development, even if again a general overestimation of the phenomenon is visible. Considering other phenomena, it can be observed that they are very limited even if the analysis has covered a rather wide range of functioning points, confirming the satisfactory result of the design process. Tip back cavitation bubbles, observed at design loading and lower cavitation number and at higher loading condition, are correctly predicted only with the RANS method, which allows to capture satisfactorily also their extension. In the case of the panel method, midchord cavitation starts for slightly lower values of the cavitation index, thus underlining a lower accuracy of the method from this point of view, as it could be expected. Sheet cavitation at tip (as an extension of the tip leakage vortex) is particularly evident at highest loading condition. In this case, both methods appear to correctly capture it. Finally, root back bubbles were observed in correspondence to the lowest cavitation number, while they are not present in both the numerical calculations. This phenomenon, however, may be at least partially ascribed to the local manufacturing of the propeller model, which presents a not completely satisfactory finishing at leading edge, which probably tends to anticipate cavitation. Moreover, the propeller geometry adopted in both calculations does not consider the effective hub/blade root fillet, resulting in a lower local profile thickness at root, which may tend to postpone this phenomenon.

6. Conclusions

In the present paper, a hybrid approach for ducted propellers design has been presented. An application of the method for the design of a propeller in a decelerating duct is reported, together with the results of an experimental campaign at the towing tank and at the cavitation tunnel, carried out in order to validate the procedure. The comparison of the numerical results and the measurements confirms the validity of the approach, which allows to obtain a propeller that, in addition to satisfy the required mechanical characteristics, is almost completely cavitation-free, apart from the presence of the tip leakage vortex. Considering also off-design points, cavitating phenomena and their extensions are satisfactorily predicted by the adopted methods within their limitations, with RANS

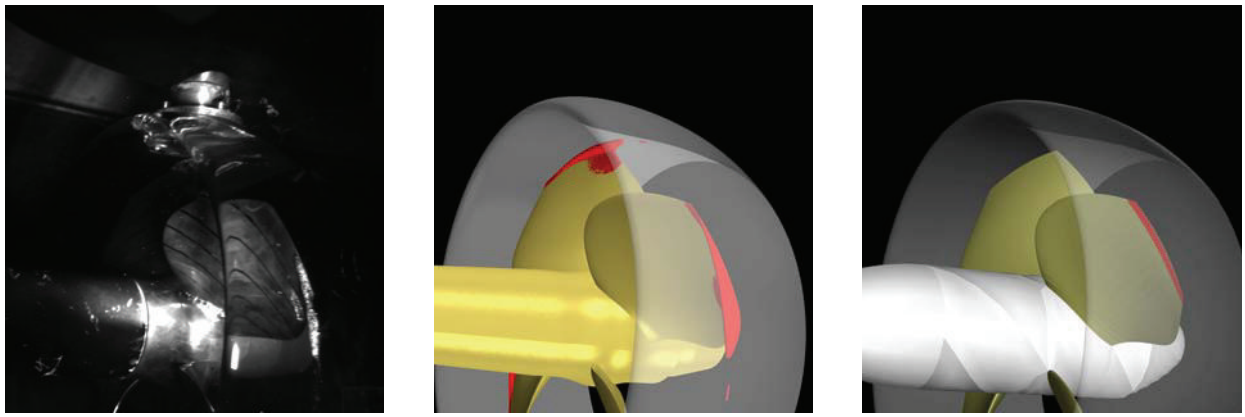

Figure 16: Observed and predicted (RANS and panel method) cavity extension. Design thrust coefficient at 80% of design cavitation index.

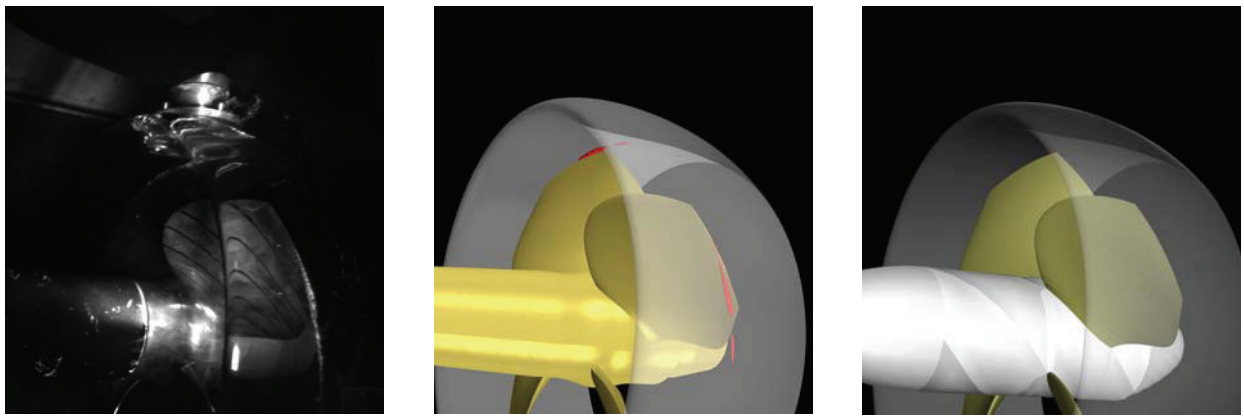

Figure 17: Observed and predicted (RANS and panel method) cavity extension. 70% of the design thrust coefficient at the design cavitation index.

solver being able to correctly capture also bubble cavitation and tip leakage vortex, even if slightly overestimating the latter: a correct capturing of the local phenomena at tip is of particular importance for a propeller in decelerating duct, whose main aim is to reduce cavitation phenomena, since it may represent an undesired source of noise. The nature of this phenomenon has to be further investigated, both numerically and experimentally, evaluating the influence of local geometrical characteristics. From this point of view, a combined application of RANS solvers, with their ability to capture the complex flow characteristics including also viscous effects, and panel methods, whose low computational requirements allow to test a very high number of solutions within reasonable time, seems to represent a very promising and convenient approach.

Acknowledgments

The authors wish to express their gratitude to Mr. Conti and Mr. Grossi, from the Hydrodynamic Department of Fincantieri Naval Vessel Business Unit, for their support and for the very pleasant discussions throughout this work.

References

[1] M. W. C. Oosterveld, *Wake Adapted Ducted Propellers*, Publication no. 345, NSMB, Wageningen, Netherlands, 1970.

[2] W. B. Coney, *A method for the design of a class of optimum marine propellers [Ph.D. thesis]*, Massachusetts Institute of Technology, Cambridge, Mass, USA, 1989.

[3] H. W. Lerbs, "Moderately loaded propellers with a finite number of blades and an arbitrary distribution of circulation," *Transaction of the Society of Naval Architects and Marine Engineers*, vol. 60, pp. 6–31, 1952.

[4] D. Bertetta, S. Brizzolara, E. Canepa, S. Gaggero, and M. Viviani, "EFD and CFD characterization of a CLT propeller," *International Journal of Rotating Machinery*, vol. 2012, Article ID 348939, pp. 1–23, 2012.

[5] D. Bertetta, S. Brizzolara, S. Gaggero, M. Viviani, and L. Savio, "CP propeller cavitation and noise optimization at different pitches with panel code and validation by cavitation tunnel measurements," *Ocean Engineering*, vol. 53, pp. 177–195, 2012.

[6] D. Bertetta, C. Bertoglio, F. Conti, C. M. Rizzo, and M. Viviani, "Cavitation tunnel tests on ducted propellers," in *Proceedings 17th International Conference on Ships and Shipping Research*, Naples, Italy, 2012.

[7] CD-Adapco, "StarCCM+, v5. 06. 10 User's manual," 2010, CD-Adapco.

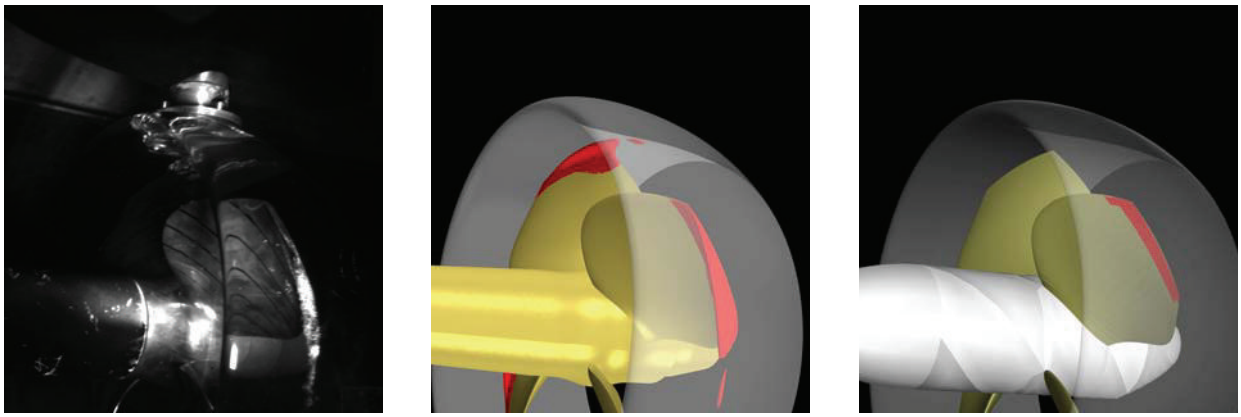

Figure 18: Observed and predicted (RANS and panel method) cavity extension. 130% of the design thrust coefficient at the design cavitation index.

[8] A. Sanchez-Caja, P. Rautaheimo, and T. Siikonen, "Simulation of incompressible viscous flow around a ducted propeller using a rans equation solver," in *Proceedings of the 23rd Symposium on Naval Hydrodynamics*, 2000.

[9] M. Abdel-Maksoud and H. J. Heinke, "Scale effects on ducted propellers," in *Proceedings of the 24th Symposium on Naval Hydrodynamics*, 2003.

[10] M. J. Hughes, *Analysis of multi-component ducted propulsors in unsteady flow [Ph.D. thesis]*, Massachusetts Institute of Technology, Cambridge, Mass, USA.

[11] J. Baltazar, J. A. C. Falcão de Campos, and J. Bosschers, "Open-water thrust and torque predictions of a ducted propeller system with a panel method," *International Journal of Rotating Machinery*, vol. 2012, Article ID 474785, 2012.

[12] J. Baltazar and J. A. C. Falcao de Campos, "On the modelling of the flow in ducted propellers with a panel method," in *Proceedings of the 1st International Symposium on Marine Propulsors (SMP '09)*, Trondheim, Norway, June 2009.

[13] J. E. Kerwin and R. Leopold, "A design theory for subcavitating propellers," 1964, Transaction SNAME, 72.

[14] J. E. Connolly, *Strength of Propellers*, Transaction of the Royal Institution of Naval Architects, 1961.

[15] L. Grossi, "PESP: un programma integrato per la progettazione di eliche navali con la teoria della superficie portante," Tech. Rep., CETENA, 1980.

[16] E. Castagneto and P. G. Maioli, "Theoretical and experimental study on the dynamics of hydrofoils as applied to naval propellers," in *Proceedings of the 7th Symposium on Naval Hydrodynamics*, 1968.

[17] S. Gaggero, D. Grassi, and S. Brizzolara, "From single to multistage marine propulsor: a fully numerical design approach," in *Proceedings of the 2nd International Symposium on Marine Propulsors*, Hamburg, Germany, 2011.

[18] S. Gaggero, D. Villa, and S. Brizzolara, "Smp workshop on cavitation and propeller performances: the experience of the University of Genova on the Potsdam propeller test case," in *Proceedings of the 2nd International Symposium on Marine Propulsors, Workshop on Propeller Performances*, Hamburg, Germany, 2011.

[19] P. VanOossanen, "Calculation of performance and cavitation characteristics of propellers including effects of non-uniform flow and viscosity," Tech. Rep., Netherland Ship Model Basin.

[20] S. Gaggero and S. Brizzolara, "A panel method for trans-cavitating marine propellers," in *Proceedings of the 7th International Symposium on Cavitation*, Ann Arbor, Mich, USA, August 2009.

[21] S. Gaggero and S. Brizzolara, "Parametric CFD optimization of fast marine propellers," in *Proceedings of the 10th International Conference on Fast Sea Transportation*, Athens, Greece, October 2009.

[22] L. Morino and C. C. Kuo, "Subsonic Potential Aerodynamic for complex configuration: a general theory," *AIAA Journal*, vol. 12, no. 2, pp. 191–197, 1974.

[23] J. Sauer and G. H. Schnerr, "Development of a new cavitation model based on bubble dynamics," *Journal of Applied Mathematics and Mechanics*, vol. 81, no. 3, pp. 561–562, 2001.

[24] C. Y. Hsin, *Development and analysis of panel methods for propellers in unsteady flow [Ph.D. thesis]*, Massachusetts Institute of Technology, Cambridge, Mass, USA, 1990.

[25] L. Savio, M. Viviani, F. Conti, and M. Ferrando, "Application of computer vision techniques to measure cavitation bubble volume and cavitating tip vortex diameter," in *Proceedings of the 7th International Symposium on Cavitation (CAV '09)*, pp. 737–748, Ann Arbor, Mich, USA, August 2009.

[26] M. Ferrando, M. Viviani, and S. Crotti, "Performance of a family of surface piercing propellers," in *Proceedings of the 2nd International Conference on Marine Research and Transportation (ICMRT '07)*, pp. C63–C70, Ischia, Italy, June 2007.

[27] C. Bertoglio, *Sviluppo di un sistema di misura per eliche intubate [M.S. thesis]*, University of Genoa, Genoa, Italy, 2011.